

Phenomenological Three-Orbital Spin-Fermion Model for Cuprates

Mostafa Sherif Derbala Aly Hussein,^{1,2} Maria Daghofer,^{3,4} Elbio Dagotto,^{1,2} and Adriana Moreo^{1,2}

¹*Department of Physics and Astronomy, University of Tennessee, Knoxville, TN 37966, USA*

²*Materials Science and Technology Division, Oak Ridge National Laboratory, Oak Ridge, TN 37831, USA*

³*Institut für Funktionelle Materie und Quantentechnologien,*

Universität Stuttgart, Pfaffenwaldring 57, D-70569 Stuttgart, Germany

⁴*Center for Integrated Quantum Science and Technology,*

University of Stuttgart, Pfaffenwaldring 57, D-70550 Stuttgart, Germany

(Dated: April 20, 2018)

A spin-fermion model that captures the charge-transfer properties of Cu-based high critical temperature superconductors is introduced and studied via Monte Carlo simulations. The strong Coulomb repulsion among d -electrons in the Cu orbitals is phenomenologically replaced by an exchange coupling between the spins of the itinerant electrons and localized spins at the Cu sites, formally similar to double-exchange models for manganites. This interaction induces a charge-transfer insulator gap in the undoped case (five electrons per unit cell). Adding a small antiferromagnetic Heisenberg coupling between localized spins reinforces the global tendency towards antiferromagnetic order. To perform numerical calculations the localized spins are considered classical, as in previous related efforts. In this first study, undoped and doped 8×8 clusters are analyzed in a wide range of temperatures. The numerical results reproduce experimental features in the one-particle spectral function and the density-of-states such as (i) the formation of a Zhang-Rice-like band with a dispersion of order ~ 0.5 eV and with rotational symmetry about wavevector $(\pi/2, \pi/2)$ at the top of the band, and (ii) the opening of a pseudogap at the chemical potential upon doping. We also observed incipient tendencies towards spin incommensurability. This simple model offers a formalism intermediate between standard mean-field approximations, that fail at finite temperatures in regimes with short-range order, and sophisticated many-body techniques such as Quantum Monte Carlo, that suffer sign problems.

PACS numbers: 74.72.-h, 74.72.Gh, 71.10.Fd, 71.15.Dx

Keywords: superconducting cuprates, charge-transfer insulator, multi-orbital models

I. INTRODUCTION

The properties of transition metal oxides (TMOs) are determined by two groups of electrons: the d -electrons at the transition metals and the p -electrons at the oxygens [1]. The d -electrons are believed to be localized and subject to strong on-site Coulomb repulsion U_d while the p -electrons are considered itinerant with a smaller Coulomb repulsion U_p . However, the d -electrons can be delocalized by hybridization with the p -electrons and, thus, the degree of hybridization, that varies with the ratio of the Coulomb repulsion to hopping amplitudes, plays an important role in determining the properties of TMOs [1]. In addition, the on-site energies ϵ_p and ϵ_d of the p and d orbitals also affect the properties of TMOs [2]. Depending on the relative value of $\Delta = \epsilon_d - \epsilon_p$, U_d , and the bandwidth W of the itinerant electrons, the latter as determined from the limit when Coulomb repulsion is turned off, the TMOs may be in various different regimes. The Mott-Hubbard regime occurs when $U_d < \Delta$ and an insulating gap opens in the d -band if it is half-filled. If $U_d > \Delta$ the system is considered to be in the charge-transfer (CT) regime. A gap defined by an electron filled p -band and an empty d -band opens when the d -band is nominally half-filled. Systems with large Hubbard repulsions but with $\Delta < W/2$ can be metallic [2]. Recently, even the case of negative charge-transfer gaps $\Delta < 0$ has been considered [3–6].

Among the most important families of TMOs are the high critical temperature superconducting cuprates. Their parent compounds are charge-transfer insulators (CTI) [2, 7], but from the theory perspective they have been studied primarily using single-orbital Hubbard or $t - J$ models because these models are simpler than more realistic multiorbital Hamiltonians that include oxygens. Using simplified one-band models is justified by the experimental observation of a single-band Fermi surface [8–11] and also by the Zhang-Rice singlet concept where the three-orbital Hubbard model is approximately mapped into an effective $t - J$ model [12]. While many properties of the cuprates have been captured by single-band models [7], several questions regarding the role of the oxygen remain. One of the main issues are the differences between the properties of doped Mott insulators, described by single-band models, and charge-transfer insulators where both the $d_{x^2-y^2}$ Cu orbital and the p_σ O orbitals are considered. Early numerical studies of three-band models did not indicate major physical differences among both approaches [13–15], but other authors have claimed that the multiorbital character plays a crucial role in the physics of the cuprates [16, 17].

The discovery of the iron-based superconductors [18–21] brought to the forefront the need to develop models and numerical approaches to deal with multi-orbital systems. In this context, effective multi-orbital spin-fermion models were developed that allowed the study of many

properties of these materials such as magnetic phases, density of states, Fermi surface, and resistivity, among others [22]. These efforts on iron pnictides and chalcogenides actually built upon the double-exchange models for manganites. The aim of the present work is to develop a spin-fermion model for the CuO_2 planes of the cuprates that can be studied with the Monte Carlo techniques previously developed for the pnictides, with the goal to understand, at least qualitatively, the role played by the O p_σ -orbitals.

A single-orbital, as opposed to multi-orbital, spin-fermion model for the cuprates was developed in the 90s [23]. In that early effort, the Cu d -band was split via a spin-spin interaction among phenomenological localized spins and the spins of the itinerant electrons, similarly as in the model proposed here. This interaction prevents the double occupancy of the Cu sites, crudely mimicking the Hubbard on-site repulsion effects. By using classical localized spins and Monte Carlo, several of the static and dynamical properties of the cuprates were reproduced showing that this avenue, that interpolates between traditional mean-field approximations and far more complicated Quantum Monte Carlo approaches, is fruitful. Magnetic incommensurability and a short-distance tendency towards d -wave pairing was observed upon doping [23, 24].

In the present effort, starting with the standard tight-binding term of the three-orbital Hubbard model for cuprates and introducing phenomenological localized spins, we will find the interaction parameters values that better reproduce the density of states (DOS) of the full Cu oxide Hamiltonian. The tight-binding term involves $3d_{x^2-y^2}$ Cu and $2p_\sigma$ ($2p_x$ or $2p_y$) orbitals of the two oxygens in the CuO_2 unit cell. As already explained, the Cu-sites Hubbard repulsion that splits the half-filled d -band will be replaced by a magnetic coupling between the spin of the itinerant electrons when at the d -orbital and Cu localized spins. A small antiferromagnetic Heisenberg coupling among nearest-neighbor localized spins enhances the global antiferromagnetic tendencies. In addition, the spins of the p -orbital electrons are coupled antiferromagnetically to their two neighboring localized spins.

In the undoped case, with five electrons per CuO_2 unit cell, it will be shown that the model leads to a charge-transfer insulator where, unexpectedly, the gap states have approximately *equal* amounts of p and d character. This is contrary to the widely held perception that holes reside primarily at the oxygens. This is also different from the one-orbital Mott insulator approach in which one single orbital contributes entirely to the states that define the gap.

Several other interesting results were obtained. For instance, long-range antiferromagnetic order, as in the parent compound of the cuprates, develops with reducing temperature. Incipient tendencies towards spin incommensurability were observed with doping. Even more importantly, a study of the one-particle spectral functions indicates that, in agreement with angular-resolved pho-

toemission (ARPES) results for the undoped cuprates, states with wavevectors $(\pm\pi/2, \pm\pi/2)$ are the first to accept doped holes. The ARPES region around these wavevectors are rotationally symmetric, with equal curvature in all directions, a feature reproduced in single-band models only after the addition of longer range hoppings, while in our approach it emerges spontaneously without fine tuning. In addition, the lowest state for electron doping has momentum $(\pi, 0)$ and $(0, \pi)$, as expected. Moreover, a Zhang-Rice-like singlet (ZRS) band spontaneously appears in the DOS, and a pseudogap at the chemical potential develops upon doping.

The paper is organized as follows: in Section II results for the DOS of the full undoped three-orbital Hubbard model are presented to guide the tuning of parameters in the proposed spin-fermion model which is introduced in Section III. Results for the DOS and the one-particle spectral functions (photoemission), as well as the magnetic structure factor, are presented in Section IV, while Section V is devoted to the conclusions.

II. CHARGE-TRANSFER REGIMES IN THE THREE-BAND HUBBARD MODEL

The band gaps and electronic structures of TMOs were described before [2] and they depend on the relationship between the charge-transfer energy Δ and the d - d Hubbard repulsion U_d . In general, if $U_d < \Delta$ the band gap of the undoped state is controlled by U_d and the system is a Mott-Hubbard insulator, while if $U_d > \Delta$ the gap is controlled by Δ and of charge-transfer nature for $\Delta > W/2$, where W is the bandwidth of the oxygen p -band [2]. However, the role of the hybridization between the d and p bands, important in cuprates, is often neglected. For this reason, first we present results for the orbital-resolved density-of-states of the undoped three-orbital Hubbard model obtained using the variational cluster approach (VCA) [13]. The Hamiltonian, in electron notation, is given by

$$H_{3\text{BH}} = H_{\text{TB}} + H_{\text{int}}, \quad (1)$$

where

$$\begin{aligned} H_{\text{TB}} = & -t_{pd} \sum_{\mathbf{i}, \mu, \sigma} \alpha_{\mathbf{i}, \mu} (p_{\mathbf{i}+\frac{\mu}{2}, \mu, \sigma}^\dagger d_{\mathbf{i}, \sigma} + h.c.) - \\ & t_{pp} \sum_{\mathbf{i}, (\mu, \nu), \sigma} \alpha'_{\mathbf{i}, \mu, \nu} [p_{\mathbf{i}+\frac{\mu}{2}, \mu, \sigma}^\dagger (p_{\mathbf{i}+\frac{\nu}{2}, \nu, \sigma} + p_{\mathbf{i}-\frac{\nu}{2}, \nu, \sigma}) + h.c.] \\ & + \epsilon_d \sum_{\mathbf{i}} n_{\mathbf{i}}^d + \epsilon_p \sum_{\mathbf{i}, \mu} n_{\mathbf{i}+\frac{\mu}{2}}^p + \mu_e \sum_{\mathbf{i}, \mu} (n_{\mathbf{i}+\frac{\mu}{2}}^p + n_{\mathbf{i}}^d), \end{aligned} \quad (2)$$

and

$$H_{\text{int}} = U_d \sum_{\mathbf{i}} n_{\mathbf{i}, \uparrow}^d n_{\mathbf{i}, \downarrow}^d + U_p \sum_{\mathbf{i}, \mu, \sigma} n_{\mathbf{i}+\frac{\mu}{2}, \uparrow}^p n_{\mathbf{i}+\frac{\mu}{2}, \downarrow}^p. \quad (3)$$

The operator $d_{\mathbf{i},\sigma}^\dagger$ creates an electron with spin σ at site \mathbf{i} of the copper square lattice, while $p_{\mathbf{i}+\frac{\hat{\mu}}{2},\mu,\sigma}^\dagger$ creates an electron with spin σ at orbital p_μ , where $\mu = x$ or y , for the oxygen located at $\mathbf{i} + \frac{\hat{\mu}}{2}$. The hopping amplitudes t_{pd} and t_{pp} correspond to the hybridizations between nearest-neighbors Cu-O and O-O, respectively, and $\langle \mu, \nu \rangle$ indicate O-O pairs connected by t_{pp} as indicated in Fig. 1. $n_{\mathbf{i}+\frac{\hat{\mu}}{2},\sigma}^p$ ($n_{\mathbf{i},\sigma}^d$) is the number operator for p (d) electrons with spin σ , and ϵ_d and ϵ_p are the on-site energies at the Cu and O sites, respectively. If $\epsilon_d = 0$ then $\Delta = \epsilon_d - \epsilon_p$, is the charge-transfer gap. The Coulomb repulsion between two electrons at the same site and orbital is U_d (U_p) for d (p) orbitals. The signs of the Cu-O and O-O hoppings due to the symmetries of the orbitals is included in the parameters $\alpha_{\mathbf{i},\mu}$ and $\alpha'_{\mathbf{i},\mu,\nu}$ and follows the convention shown in Fig. 1. Finally, μ_e is the electron chemical potential.

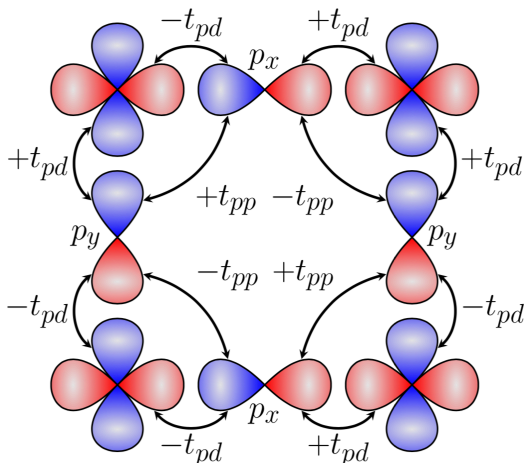


FIG. 1: (color online) Schematic drawing of the Cu $d_{x^2-y^2}$ orbitals at the copper sites of the square lattice, with the sign convention indicated by the colors (red for + and blue for -). The oxygen p_σ orbitals with their corresponding sign convention are also shown, located at the Cu-O-Cu bonds. The sign convention for the t_{pd} and t_{pp} hoppings is also indicated.

The orbital-resolved DOS in the electron representation for the accepted values of $U_d = 8t$ [13, 14] and $U_p = 3t$ (where $t = t_{pd}$ is the energy unit) is in Fig. 2 (a). The effect of the Coulomb repulsion on the DOS can be understood by comparing with the tight-binding band dispersion in Fig. 3. The spectral weight associated to the portion of the band above the chemical potential in Fig. 3 appears to the right of the chemical potential in Fig. 2. It is clear that the gap where the chemical potential is located in Fig. 2 results mostly from the split, due to U_d , of the top band in Fig. 3 which, as shown in the figure, arises mostly from the d orbitals (that in the electron picture are on top). In the non-interacting limit, this band has a small oxygen content due to the hybridization t_{pd} and it has a similar dispersion to the tight-binding band of the single-band Hubbard model when $t' = -0.3t$ and $t'' = 0.2t$ hoppings are added [13, 25, 26]. Thus,

the gap opening in the top band is “captured” by the single-particle model with $U = 8t$ [13].

As shown in Fig. 2 (a), the charge-transfer gap where the chemical potential resides at $U_d/t = 8$ is about $2t$, similar in magnitude to the Mott gap of the single-band Hubbard model with $U/t = 8$ [7, 27]. Naively, the DOS gap would be expected to be proportional to U , but in both cases screening effects reduce the gap. The main qualitative difference, though, lies in the orbital composition of the band. As shown in Fig. 2 (a), the spectral weight occupied by electrons immediately at the left of the chemical potential has a 50%-50% $p-d$ orbital composition indicating its charge-transfer character (red and blue curves have almost identical weight). This is due to the additional hybridization effects caused by the strong Coulomb interaction that affects the spectral weight from the p tight-binding bands. On the other hand, the spectral weight at the right of the chemical potential in Fig. 2 (a) is mostly of d -character i.e. when electrons are added they populate d -Cu orbitals.

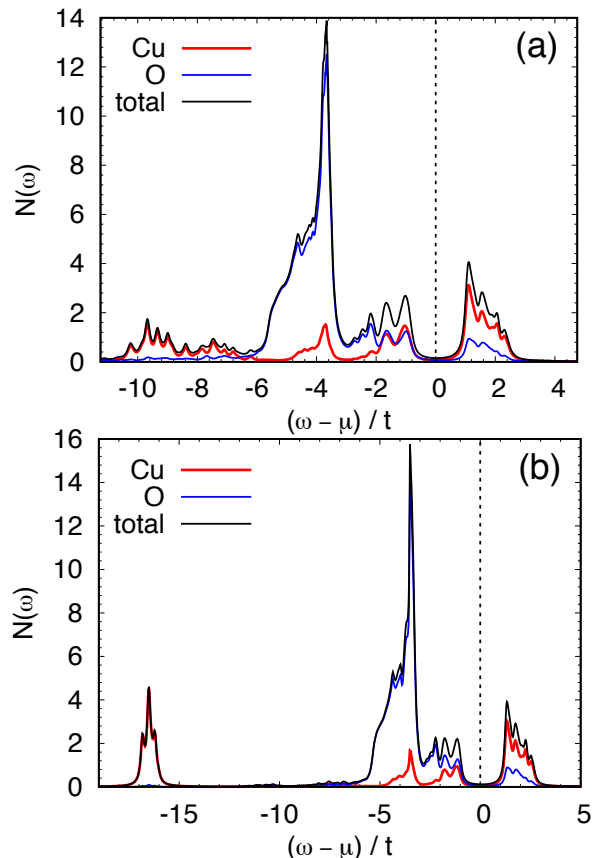


FIG. 2: (color online) Orbital-resolved density-of-states for the full three-band Hubbard model with the parameters used before in Ref. [13] where $t_{pd} = t$ is the unit of energy and $t_{pp} = 0.5t$, $\Delta = 3t$, and $U_p = 3t$. Panel (a) corresponds to $U_d = 8t$ while panel (b) to $U_d = 16t$. The dashed line indicates the chemical potential in the undoped case with one hole (five electrons) per CuO_2 unit cell. Results are shown in the electron notation.

Note also that a small amount of spectral weight, almost 100% of d character, has been transferred to lower energy (in the electron picture) in the interval $-10 < (\omega - \mu)/t < -6$. This weight was previously identified by some authors as the “lower Hubbard band” (LHB) [4] although a well-defined LHB is not sharply developed at the value of U_d considered realistic. In fact, we found that to develop a well-defined LHB, as in an extreme charge-transfer system [2], a U_d as large as $16t$ is required. The DOS in this situation is in Fig. 2 (b). The LHB is located at $(\omega - \mu)/t \approx -16$ and it has 100% d character. Now the separation between the upper and lower Hubbard bands is approximately U_d while the charge-transfer gap is only slightly reduced. Still for the two values of U_d presented in Fig. 2 it is clear that due to the $p - d$ hybridization, arising from the combined effect of interorbital hopping and Coulomb interaction, the states that define the charge-transfer gap have *mixed* orbital character [28]. This indicates that doped holes will go both into the oxygens *and* the coppers since the spectral weight is comparable among p and d orbitals. In summary, the deviations clarified in this section from the simplistic view of either purely Hubbard or purely charge-transfer gap materials were not emphasized before in the literature, increases the level of complexity of the system, and will be an important feature that we will try to capture in the effective model presented next. We conclude this section stating that cuprates are not sharply “charge-transfer” insulators but they reside at the intersection between the Hubbard and charge-transfer families.

III. EFFECTIVE THREE-BAND MODEL FOR CuO_2 PLANES

The starting point for the effective model that we will develop is the tight-binding portion of the three-band Hubbard model given in Eq. 2 with $t_{pd} = 1.3$ eV and $t_{pp} = 0.65$ eV, on-site energy $\epsilon_p = -3.6$ eV [14], and a $\Delta = \epsilon_d - \epsilon_p$ which is positive ($\epsilon_d = 0$) [29].

Note that in the electron representation the undoped case is characterized by one hole at the coppers and no holes at the oxygens, which corresponds to five electrons per CuO_2 unit cell (the maximum possible electronic number in three orbitals is six). The orbital-resolved tight-binding bands along the $\Gamma - X - M - \Gamma$ path in the Brillouin zone calculated on a 100×100 square lattice (with coppers at the sites of the lattice) is in Fig. 3. The dashed black line is the chemical potential for electronic density $\langle n \rangle = 5$ and the corresponding Fermi surface is in the inset. An analysis of the orbital composition of each of the three bands, shown by the color palette in the figure, indicates that the top band is purely d at the Γ point and becomes hybridized with the p orbitals so that its d content is 78% at X and 56% at M. The two bottom bands have pure p character at the Brillouin zone center. The middle band achieves 43% d character at M, while the lower band has 21% d character at X. Note that

the tight-binding Fermi surface, shown in the inset, has the qualitative form expected in the cuprates. However, its orbital content is about 75% d only, showing that the oxygen component is not negligible even if only one band crosses the Fermi level.

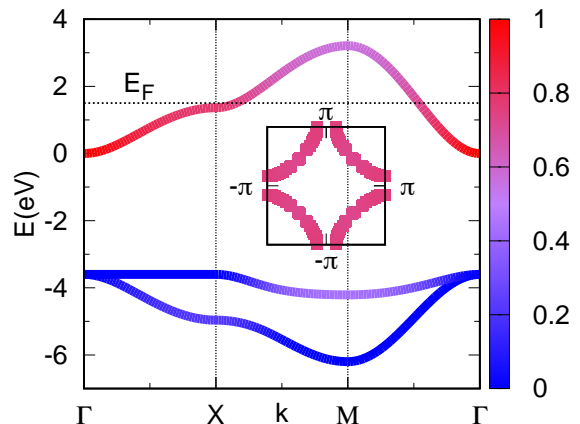


FIG. 3: (color online) Band dispersion for the tight-binding term of the CuO_2 Hamiltonian. The orbital content is displayed with red (blue) indicating d (p) character. The dashed line indicates the position of the chemical potential (or Fermi level E_F) at density $\langle n \rangle = 5$ (undoped case). The Fermi surface at this density is in the inset. Colors indicate the orbital content of the bands, with the palette on the right denoting the weight of the d component (e.g. 1 means 100% copper d , and the oxygen weight is simply one minus the copper weight).

The interaction term in the spin-fermion model is purely *phenomenological*, as in all spin-fermion models in previous literature. It is introduced to prevent double occupancy in the d orbitals by creating lower and upper bands, while spectral weight originating in the p orbitals remains in the middle, in such a way that a charge-transfer insulator results for five electrons per unit cell. To achieve these goals, we introduce phenomenological localized spins at the Cu sites. These on-site spins will be coupled via an antiferromagnetic coupling J_{Sd} to the spins of the mobile d -electrons at the same site via

$$H_{\text{Sd}} = J_{\text{Sd}} \sum_{\mathbf{i}} \mathbf{S}_{\mathbf{i}} \cdot \mathbf{s}_{\mathbf{i}}, \quad (4)$$

where $\mathbf{S}_{\mathbf{i}}$ denotes the localized spins at \mathbf{i} , $\mathbf{s}_{\mathbf{i}} = d_{\mathbf{i},\alpha}^\dagger \vec{\sigma}_{\alpha\beta} d_{\mathbf{i},\beta}$ is the spin of the mobile d -electrons, and $\vec{\sigma}_{\alpha\beta}$ are Pauli matrices. Since this term is phenomenological, in principle the coupling between localized and itinerant spins can be either anti- (AF) or ferromagnetic (FM) since in the AF (FM) case the lower d -band will contain electrons with spins antiparallel (parallel) to the localized spins. For the classical localized spins used here, the results are independent of the sign of J_{Sd} and we will simply consider the AF coupling as our convention. Note that in the absence of electronic hopping this interaction would lead to a half-filled d -band and totally filled p -bands for the overall density $\langle n \rangle = 5$ per CuO_2 cell.

To enhance further the tendency towards antiferromagnetic order in the undoped case, as in real undoped cuprates, an antiferromagnetic Heisenberg coupling J_{AF} between the localized spins is also introduced via

$$H_{AF} = J_{AF} \sum_{\mathbf{i}} \mathbf{S}_{\mathbf{i}} \cdot \mathbf{S}_{\mathbf{i}}. \quad (5)$$

Finally, a coupling J_{Sp} between the localized spins and the p -electrons spins at each of the four neighboring oxygens is added (introducing effectively magnetic frustration upon doping)

$$H_{Sp} = J_{Sp} \sum_{\mathbf{i}, \hat{\mu}} \mathbf{S}_{\mathbf{i}} \cdot \mathbf{s}_{\mathbf{i}+\frac{\hat{\mu}}{2}}, \quad (6)$$

where $\hat{\mu} = \pm\hat{x}$ or $\pm\hat{y}$ and $\mathbf{s}_{\mathbf{i}+\frac{\hat{\mu}}{2}} = p_{\mathbf{i}+\frac{\hat{\mu}}{2}, \mu, \alpha}^{\dagger} \vec{\sigma}_{\alpha\beta} p_{\mathbf{i}+\frac{\hat{\mu}}{2}, \mu, \beta}$.

Thus, the spin-fermion (SF) Hamiltonian defined here is given by four terms as

$$H_{SF} = H_{TB} + H_{Sd} + H_{AF} + H_{Sp}. \quad (7)$$

This phenomenological Hamiltonian we propose is reminiscent of the model in Ref. [17] except that they work in the limit where the d electrons are fully localized and only contribute their magnetic degree of freedom.

The computational simplification that allows the numerical study of our Hamiltonian is that the localized spins are assumed classical [30]. With this approximation, the full H_{SF} can be studied with the same Monte Carlo (MC) procedure widely employed before for the pnictides [22] and double-exchange manganites [31].

To select the values of the couplings, we studied the properties of the model for a variety of parameters finding the combination that better reproduced some experimental properties of the cuprates and the results in Fig. 2. In Fig. 4, we present the orbital-resolved density-of-states for $J_{AF} = 0.1$ eV, $J_{Sp} = 1$ eV, and several values of J_{Sd} . At $J_{Sd} = 0$ in panel (a), the chemical potential (vertical dashed line) is in the middle of the upper band of mostly d -character and the system is metallic. However, at $J_{Sd} = 2$ eV, panel (b), the upper band is split. Now the undoped system is an insulator with the chemical potential inside a gap. While the gap is similar to the charge-transfer gap of the cuprates $\Delta \approx 2$ eV [32], note that the band to the left of μ has primarily d -character. By increasing further J_{Sd} both the magnitude of the insulating gap and the p composition of the band below μ increases. We found that for $J_{Sd} = 3$ eV, panel (c), the d and p orbitals contribute *equally* to the density-of-states just below the chemical potential as in the three-orbital Hubbard model discussed before with $U_d = 8t$ [Fig. 2 (a)], and the charge-transfer gap is about 3 eV. If J_{Sd} continues to increase, then the d spectral weight continues to be redistributed and for $J_{Sd} = 4$ eV [panel (d)] there is more p than d weight to the left of the chemical potential, but no sharp lower-band has yet developed (equivalent to a Hubbard lower-band). This lower band develops when $J_{Sd} = 8$ eV as shown in panel (e). Finally, for extreme

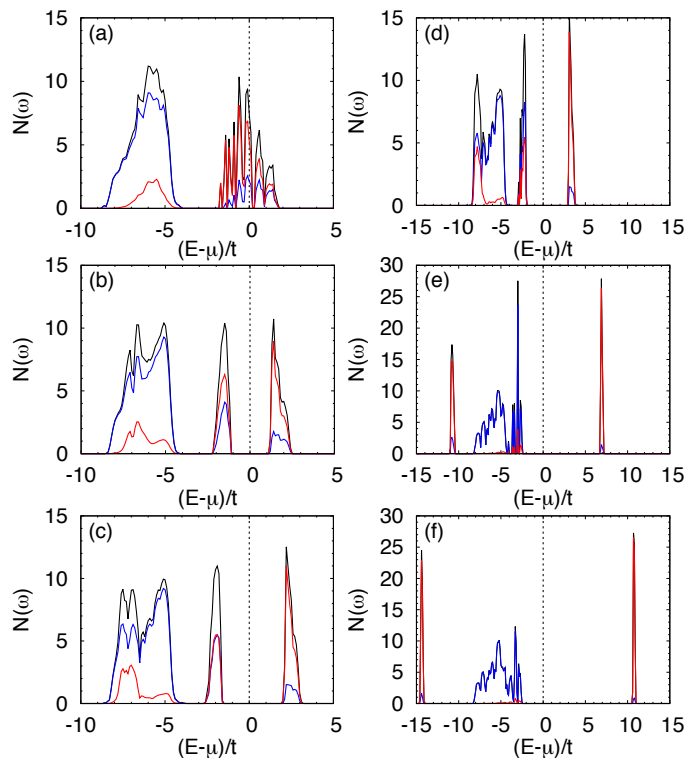


FIG. 4: (color online) Orbital-resolved density-of-states for the spin-fermion model with $J_{AF} = 0.1$ eV and $J_{Sp} = 1$ eV. The various panels correspond to (a) $J_{Sd} = 0$, (b) $J_{Sd} = 2$, (c) $J_{Sd} = 3$, (d) $J_{Sd} = 4$, (e) $J_{Sd} = 8$, and (f) $J_{Sd} = 12$ (all in eV units). Results are for the undoped case, i.e. $\langle n \rangle = 5$ and were obtained using an 8×8 lattice at temperature $T \sim 120$ K. The d (p) spectral weight is in red (blue) while the total spectral weight is indicated by the black line. The chemical potential is at the vertical dashed line.

values, such as $J_{Sd} = 12$ eV in panel (f), the $p-d$ hybridization is removed and the upper and lower d -bands surround the pure p bands. After this analysis, we set $J_{Sd} = 3$ eV as the value that may better capture the properties of the cuprates.

We observed that if the signs of the couplings J_{Sd} and J_{Sp} are simultaneously reversed, turning both couplings FM, the results are the same except that the up and down spins are interchanged since the only modification in the Hamiltonian is that $\sigma \rightarrow -\sigma$. However, if only the sign of one of the couplings is changed, for example $J_{Sd} = -3$ eV, the results are different and the system develops phase separation (details not shown). For this reason only AF couplings between the itinerant and the localized spins will be considered here.

The calculations shown below were performed using squared 8×8 clusters with periodic boundary conditions (PBC). These lattice sizes are larger than those accessible to study the three-band Hubbard model either via quantum Monte Carlo [33–35] or DMRG [36]. During the simulation the localized spins $\mathbf{S}_{\mathbf{i}}$ evolve via a standard Monte Carlo procedure, while the resulting single-particle Hamiltonian for the itinerant p and d electrons

is exactly diagonalized [31]. The present simulations are performed at inverse temperature $\beta = (k_B T)^{-1}$ ranging from 10 to 400 in units of eV^{-1} , or temperature T from 1200 K to 30 K [37]. Reaching such low temperatures is an advantage of the present approach because for Hubbard model quantum Monte Carlo studies can only be performed at high temperatures due to the “sign problem” while DMRG can only be performed at zero temperature and ladder-like cylindrical geometries.

IV. RESULTS

A. Density of States and Band Structure

The DOS for the undoped case ($\langle n \rangle = 5$) was calculated for β/t ranging from 10 to 400 and $t = 1$ eV. Because of the J_{Sd} interaction, the width of the spectrum increases from 9.5 eV in the non-interacting case (Fig. 3) to about 12 eV at $J_{\text{Sd}} = 3$ eV [Fig. 4 (c)] and in this case, as shown in Fig. 5 (a), the chemical potential is in a charge-transfer gap. The dispersion of the bands is reduced as the temperature decreases rendering the features in the DOS sharper. In addition, to the left of the chemical potential there are two structures, and the peak closest to the chemical potential could be identified with a band resembling the Zhang-Rice singlet (ZRS) band.

The photoemission one-particle spectral functions $A(\mathbf{k}, \omega)$ were also calculated and their projection along selected directions of the Brillouin zone are shown in Fig. 6 (a) at our lowest temperature $\beta = 400$ eV^{-1} (i.e. $T \sim 30$ K). Below the chemical potential, the closest state in the ZRS-like band is at momentum $(\pi/2, \pi/2)$ (half-point in the $M - \Gamma$ and $X - Y$ directions) indicating that this will be the momentum of a doped hole, as expected in the cuprates [7, 13]. On the other hand, the lowest states in the upper band are at $X = (\pi, 0)$ and $Y = (0, \pi)$ suggesting that doped electrons will have these momenta, as also observed before [13]. Remarkably, we have found that the maximum around $(\pi/2, \pi/2)$ is considerably *symmetric* along $\Gamma - M$ and $X - Y$, i.e. with a similar down curvature, a characteristic of the dispersion observed in early photoemission experiments for the undoped $\text{Sr}_2\text{CuO}_2\text{Cl}_2$ cuprate [10] that only can be reproduced in one-band Hubbard and $t - J$ models by adding diagonal and second nearest-neighbor hoppings [38, 39]. In fact, comparing with the experimental data [10] the dispersion in our results along the directions $\Gamma - M$ and $X - Y$ is 0.5 and 0.8 eV, respectively, as shown in panels (a) and (b) of Fig. 7, close to the 0.3-0.4 eV observed experimentally [10]. Note that in the single-band models with only nearest-neighbor hoppings the dispersion along $X - Y$ is very flat [10, 38, 39] while a stronger dispersion is established along that direction in the spin-fermion model because of the p -orbitals.

The orbital-resolved DOS is displayed in Fig. 6 (b). Because the conduction band is mostly d in character, doped electrons will be located into d -orbitals, while the

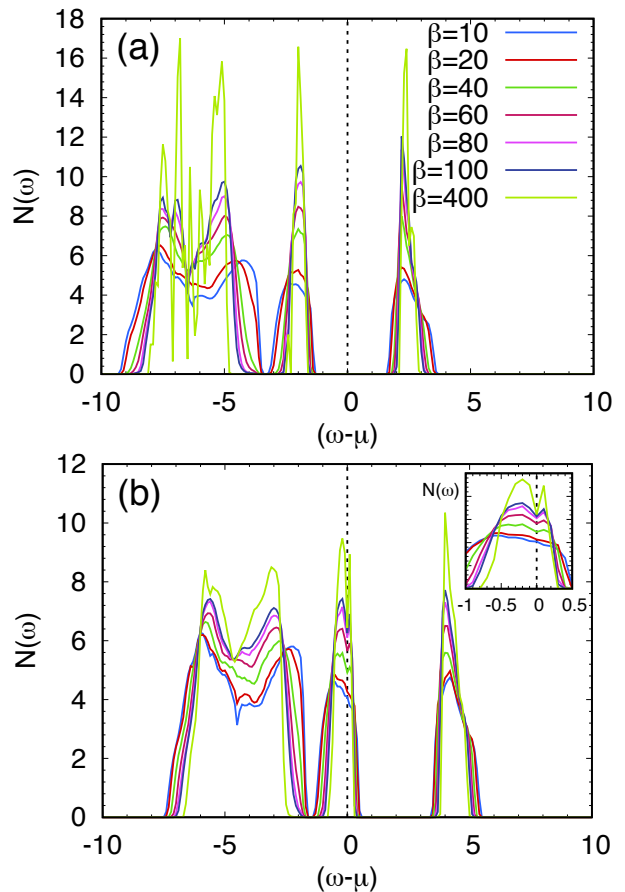


FIG. 5: (color online) Spin-fermion model density-of-states with $J_{\text{Sd}}=3$, $J_{\text{Sp}}=1$, and $J_{\text{AF}}=0.1$ (all in eV) using an 8×8 lattice and several inverse temperatures ($\beta = 400$ corresponds to $T \sim 30$ K while $\beta = 10$ to $T \sim 1200$ K). (a) corresponds to the undoped case $\langle n \rangle = 5$ while (b) is at 25% doping $\langle n \rangle = 4.75$ (16 holes). The inset shows the pseudogap in the ZRS band at the chemical potential.

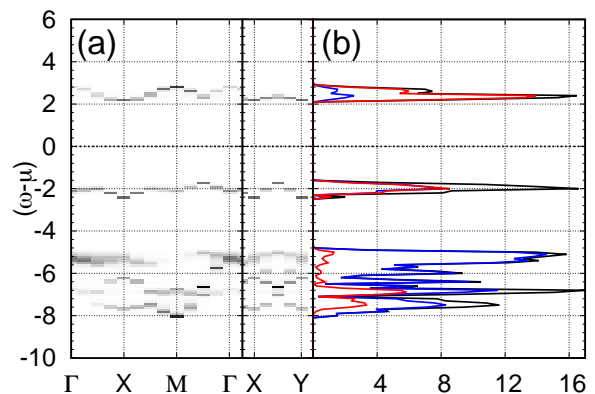


FIG. 6: (color online) (a) Spectral function $A(\mathbf{k}, \omega)$ along selected directions in the Brillouin zone for the spin-fermion model with $J_{\text{Sd}}=3$, $J_{\text{Sp}}=1$, and $J_{\text{AF}}=0.1$ (all in eV) using an 8×8 lattice at low temperature $T \sim 30$ K in the undoped case. (b) Orbital-resolved DOS states with parameters as in panel (a). The orbital spectral weight is indicated in red (blue) for the d (p) electrons. Black is the total.

ZRS-like band is a 50-50 mix of $p-d$ character as discussed before. This indicates that, due to the additional hybridization caused by the interactions, doped holes distribute evenly among oxygen and copper atoms, an unusual concept in cuprates where it is widely assumed that holes have entirely oxygen character. In addition, we have observed that the orbital decomposition supports the identification of the charge-transfer band with a ZRS-like band since its p -character vanishes approaching Γ , Fig. 8 (b), while its d -character is small close to M , see panel (a), in agreement with the phase factor of the ZRS wave function [13, 40, 41]. This is similar to results obtained for the three-band Hubbard model [13] except that the dispersion of the ZRS observed in this previous VCA study is of order $t_{pd} \approx 1.3$ eV, slightly larger than the dispersion observed experimentally and in the spin-fermion model. Finally, in Fig. 6 (b) there is a lower band, mostly of p -character with a small d contribution, similar to the lower spectral weight, observed in the three-orbital Hubbard model for $U_d = 8t$ in Fig. 2 (a).

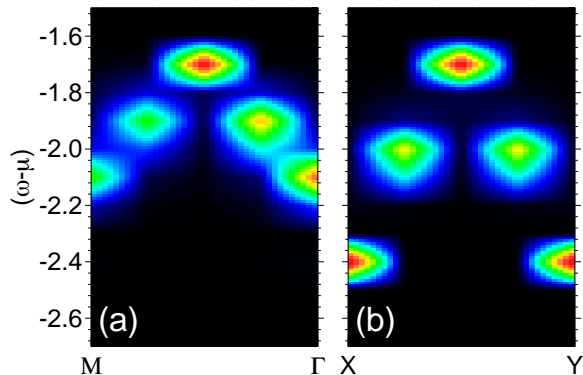


FIG. 7: (color online) Spectral function $A(\mathbf{k}, \omega)$ for the ZRS-like band using the spin-fermion model with $J_{Sd}=3$, $J_{Sp}=1$, and $J_{AF}=0.1$ (all in eV) on an 8×8 lattice at low temperature $T \sim 30$ K in the undoped case. (a) are results along the $M-\Gamma$ direction in the Brillouin zone, while (b) is same as (a) but along the $X-Y$ direction.

Consider now 25% hole doping. We focus on this doping to compare with results for the three-orbital Hubbard model obtained using density functional theory combined with the dynamical mean-field theory (LDA+DMFT) [4, 42]. The DOS at different temperatures is in Fig. 5 (b). An important difference with the undoped case [panel (a)] is that as the temperature decreases the charge-transfer band develops a pseudogap at the chemical potential (inset of the figure). In Ref. [42] the spectral weight to the right of the chemical potential was identified with the quasiparticle, while the spectral weight to the left with the incoherent part of the Zhang-Rice singlet. Our main features of the DOS are in qualitative agreement with those observed in the LDA-DMFT study of the three-orbital Hubbard model: the evolution with doping of the ZRS band shows the split of the band into a quasiparticle and an incoherent band. This be-

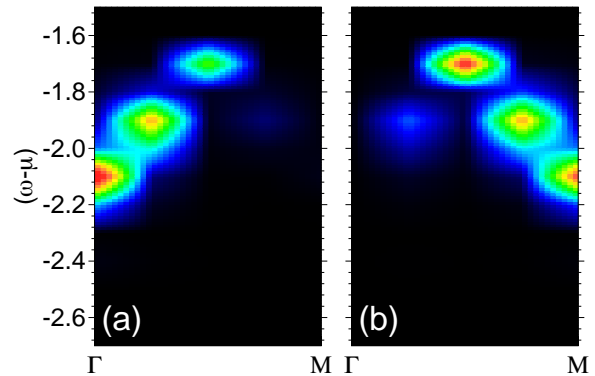


FIG. 8: (color online) Orbital-resolved spectral function $A(\mathbf{k}, \omega)$ for the ZRS-like band shown along the $\Gamma-M$ direction in the Brillouin zone. We use the spin-fermion model with $J_{Sd}=3$, $J_{Sp}=1$, and $J_{AF}=0.1$ (all in eV) on an 8×8 lattice at low temperature $T \sim 30$ K and in the undoped case. Panel (a) are results for the d -orbital spectral weight, and (b) for the p -orbitals spectral weight.

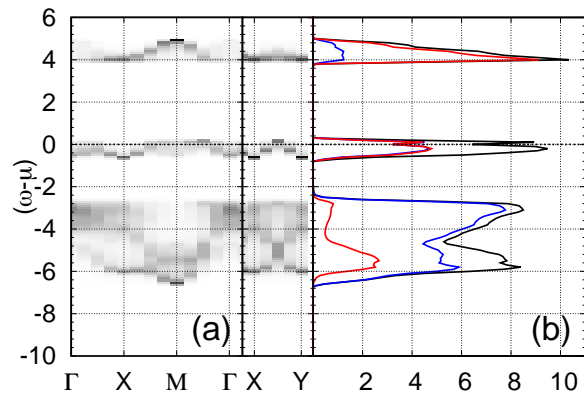


FIG. 9: (color online) (a) Spectral function $A(\mathbf{k}, \omega)$ shown along selected directions in the Brillouin zone for the spin-fermion model with $J_{Sd}=3$, $J_{Sp}=1$, and $J_{AF}=0.1$ (all in eV) on an 8×8 lattice, at low temperature $T \sim 30$ K, and with 25% hole doping. (b) Orbital-resolved DOS corresponding to panel (a). The orbital spectral weight is indicated in red (blue) for the d (p) electrons. Black is the total.

havior is observed in Fig. 9 along the main directions in the Brillouin zone in panel (a), while in (b) the DOS pseudogap develops.

Figure 10 (a) shows that the dispersion is no longer symmetric about $(\pi/2, \pi/2)$ along the nodal direction $\Gamma - M$ as in the undoped case. The quasiparticle peak is below the chemical potential at Γ and above at M , while incoherent weight remains below μ . This feature is crudely reminiscent of the “waterfall” observed experimentally in the cuprates [43, 44]. In addition, see panel (b) of the figure, the quasiparticle crosses twice the chemical potential along $X - Y$ defining a Fermi surface.

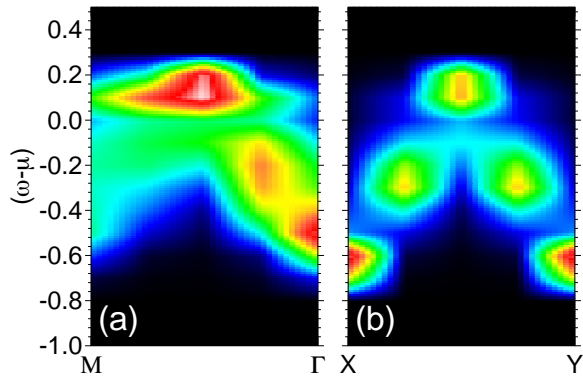


FIG. 10: (color online) (a) Spectral function $A(\mathbf{k}, \omega)$ corresponding to the ZRS-like band shown along the M- Γ direction in the Brillouin zone for the spin-fermion model with $J_{Sd}=3$, $J_{Sp}=1$, and $J_{AF}=0.1$ (all in eV) using an 8×8 lattice at low temperature $T \sim 30$ K and for 16 doped holes. (b) same as (a) but for the X - Y direction.

B. Magnetic Properties

Consider now the magnetic properties of the model. In the undoped case, the system develops long-range antiferromagnetic order in our finite system. The real-space spin-spin correlation functions between the localized spins are measured versus distance and their Fourier transform provides the static magnetic structure factor $S(\mathbf{k})$. In Fig. 11, $S(\mathbf{k})$ is shown for various inverse temperatures β and presented along representative directions in the Brillouin zone. The sharp peak is correctly located at (π, π) and its value increases as the temperature decreases, as expected. The inset shows $S(\mathbf{k})$ at $\mathbf{k} = (\pi, \pi)$ varying temperature. A robust antiferromagnetic order starts to develop between 200 K and 500 K, in rough quantitative agreement with the real Néel temperature $T_N \approx 300$ K in the cuprates [7]. In the spin-fermion model, there is a natural tendency towards antiferromagnetism due to the nesting of the non-interacting Fermi surface, but the addition of a small antiferromagnetic Heisenberg coupling J_{AF} between the localized spins further stabilizes the expected antiferromagnetic order in the undoped case. The electrons in the Cu d -orbitals are strongly coupled to the localized spins and their spin correlations follow the behavior of the classical spin correlations, as shown in the inset of the figure. As a consequence, in what follows it is sufficient to focus on the behavior of the classical spins.

Upon doping, the antiferromagnetic interaction between the electrons in the p_σ orbitals located at the oxygens and the localized spins at the coppers introduces magnetic frustration. This slightly affects the antiferromagnetic order as observed in the curves for different dopings in Fig. 12. The intensity of the peak at $\mathbf{k} = (\pi, \pi)$ decreases, while the weight of $S(\mathbf{k})$ at $\mathbf{k} = (\pi, 3\pi/4)$ increases, as shown in Fig. 12 where $S(\mathbf{k})$ is presented

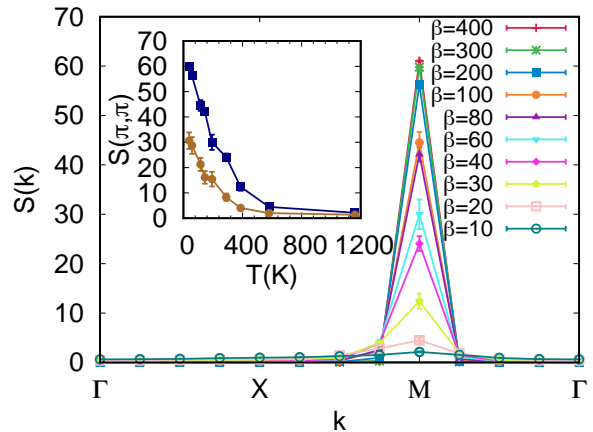


FIG. 11: (color online) Static magnetic structure factor $S(\mathbf{k})$ for the localized spins along representative directions in the Brillouin zone for the undoped spin-fermion model with $J_{Sd}=3$, $J_{Sp}=1$, and $J_{AF}=0.1$ (all in eV) using an 8×8 lattice at various values of the inverse temperature ($\beta = 400$ corresponds to $T \sim 30$ K while $\beta = 10$ to $T \sim 1200$ K). The inset shows the evolution of the structure factor at $\mathbf{k} = (\pi, \pi)$ vs temperature for the classical spins (squares) and for the spins of the electrons in the d -orbitals (circles). The quantum values have been multiplied by 5 for the sake of comparison with the results for the classical spins.

at temperature $T \sim 120$ K along representative directions in the Brillouin zone for different electronic densities. The increasing transference of weight to $(\pi, 3\pi/4)$ with hole doping captures qualitatively the expected trend towards the well-known magnetic incommensurability of the cuprates [45–47] at momentum $(\pi, \pi - \delta)$ and $(\pi - \delta, \pi)$. Experimental evidence has indicated that this incommensurability is related to stripe structures either static or dynamical [48] and more recently the possibility of states with intertwined spin, charge, and superconducting orders was also proposed [49]. The study of the possible existence of stripes, ZRS structures, high-spin polarons, and intertwined states in the ground state upon doping are future projects that can be addressed via the three-orbital spin-fermion model introduced here.

V. CONCLUSIONS

In this publication, a phenomenological three-orbital model that reproduces the charge-transfer properties of superconducting cuprates was introduced. The notorious difficulty to incorporate the electronic Coulomb repulsion of the multiorbital Hubbard model was alleviated by introducing antiferromagnetic interactions between the spins of the electrons in the three itinerant orbitals and phenomenological spins located at the coppers. The interaction of the d -electrons with the localized spins effectively induces a gap in the half-filled d -band and prevents double occupancy, similarly as the Hund interaction does in double-exchange models for manganites. Consider-

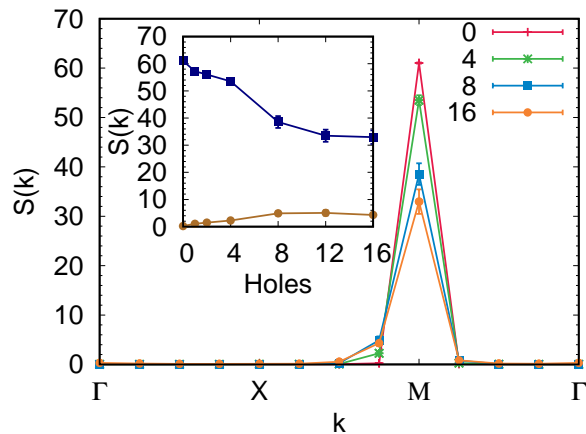


FIG. 12: (color online) Static magnetic structure factor $S(k)$ for the localized spins along representative directions in the Brillouin zone for the spin-fermion model with $J_{Sd}=3$, $J_{Sp}=1$, and $J_{AF}=0.1$ (all in eV) using an 8×8 lattice at temperature $T \sim 120$ K and for the indicated number of holes. The inset shows the evolution of $S(\pi, \pi)$ (squares) and $S(\pi, 3\pi/4)$ (circles) at $T \sim 120$ K varying the number of doped holes as indicated.

ing the localized spins as classical, as in similar models for manganites [31], one-orbital cuprates [23], and iron-based superconductors [22], the Hamiltonian becomes quadratic in the fermionic fields and it can be studied by classical Monte Carlo combined with the diagonalization of the effective single-particle quantum Hamiltonian. This process allows the study of a three-orbital Hubbard models and, moreover, the full range of temperatures can be explored.

Several features of the band structure experimentally

observed in the cuprates are well-reproduced by this simplified new model, such as the development of a charge-transfer gap in the undoped case framed by a conduction band of mostly d -character with minima at momentum $(\pi, 0)$ and $(0, \pi)$ and a ZRS-like band with a 50/50 contribution from p and d orbitals with a maximum at $(\pi/2, \pi/2)$. In addition, the band dispersion about the maximum is symmetric along $\Gamma - M$ and $X - Y$ in the Brillouin zone, an experimental property of the cuprates that is not captured by single orbital models unless t' and t'' hoppings are added. Upon doping, a pseudogap in the ZRS band develops at the chemical potential and spectral features resembling the “waterfall” are observed.

The correct magnetic properties are also captured by the spin-fermion model that displays clear tendencies towards long-range antiferromagnetic order in the undoped case. It also starts to show incipient indications of incommensurability along $(\pi - \delta, \pi)$ and $(\pi, \pi - \delta)$ in the doped case. These features upon doping, which may originate in stripes or intertwined order and that may require cylindrical boundary conditions for their stabilization, can only be seen clearly using larger clusters and they will be the subject of future work.

VI. ACKNOWLEDGMENTS

Discussions with C.B. Bishop are acknowledged. E.D. and A.M. were supported by the US Department of Energy, Office of Basic Energy Sciences, Materials Sciences and Engineering Division. M.H. was supported by the National Science Foundation, under Grant No. DMR-1404375. M.D. was supported by the Deutsche Forschungsgemeinschaft, via the Emmy-Noether program (DA 1235/1-1) and FOR1807 (DA 1235/5-1).

-
- [1] J.B. Goodenough, Magnetism and the Chemical Bond, Interscience Publ., New York-London, 1963.
 - [2] J.G. Zaanen, G.A. Sawatzky, and J.W. Allen, Phys. Rev. Lett. **55**, 418 (1985).
 - [3] D. Khomskii, arXiv:10101164.
 - [4] L. de’ Medici, X. Wang, M. Capone, and A.J. Millis, Phys. Rev. B **80**, 054501 (2009).
 - [5] L. Fratino, P. Sémon, G. Sordi, and A.-M. S. Tremblay, Phys. Rev. B **93**, 245147 (2016).
 - [6] V. Bisogni, S. Catalano, R.J. Green, M. Gibert, R. Scherwitzl, Y. Huang, V. N. Strocov, P. Zubko, S. Balandeh, J.-M. Triscone, G. Sawatzky, and T. Schmitt, Nature Communications **7** 13017 (2016).
 - [7] E. Dagotto, Rev. Mod. Phys. **66**, 763 (1994) and references therein.
 - [8] Z.-X. Shen, J. W. Allen, J. J. Yeh, J. -S. Kang, W. Ellis, W. Spicer, I. Lindau, M. B. Maple, Y. D. Dalichaouch, M. S. Torikachvili, J. Z. Sun, and T. H. Geballe, Phys. Rev. B **36**, 8414 (1987).
 - [9] J. W. Allen, C. G. Olson, M. B. Maple, J.-S. Kang, L. Z. Liu, J.-H. Park, R. O. Anderson, W. P. Ellis, J. T. Markert, Y. Dalichaouch, and R. Liu, Phys. Rev. Lett **64**, 595 (1990).
 - [10] B.O. Wells, Z. -X. Shen, A. Matsuura, D. M. King, M. A. Kastner, M. Greven, and R. J. Birgeneau, Phys. Rev. Lett **74**, 964 (1995).
 - [11] A. Damascelli, Z. Hussain, and Z.-X. Shen, Rev. Mod. Phys. **75**, 473 (2003).
 - [12] F.C. Zhang and T.M. Rice, Phys. Rev. B **37**, 3759 (1988).
 - [13] E. Arrigoni, M. Aichhorn, M. Daghofer, and W. Hanke, New Journal of Physics **11** 055066 (2009).
 - [14] Mark S. Hybertsen, Michael Schlüter, and Niels E. Christensen, Phys. Rev. B **39**, 9028 (1989).
 - [15] S. B. Bacci, E. R. Gagliano, R. M. Martin, and J. F. Annett, Phys. Rev. B **44**, 7504 (1991).
 - [16] V. J. Emery, Phys. Rev. Lett. **58**, 2794 (1987).
 - [17] B. Lau, M. Berciu, and G. A. Sawatzky, Phys. Rev. Lett. **106**, 036401 (2011).
 - [18] Y. Kamihara, T. Watanabe, M. Hirano, and H. Hosono, J. Am. Chem. Soc. **130**, 3296 (2008).
 - [19] G. F. Chen, Z. Li, G. Li, J. Zhou, D. Wu, J. Dong, W. Z. Hu, P. Zheng, Z. J. Chen, H. Q. Yuan, J. Sin-

- gleton, J. L. Luo, and N. L. Wang, Phys. Rev. Lett. **101**, 057007 (2008).
- [20] G. F. Chen, Z. Li, D. Wu, G. Li, W. Z. Hu, J. Dong, P. Zheng, J. L. Luo, and N. L. Wang, Phys. Rev. Lett. **100**, 247002 (2008).
- [21] H.-H. Wen, G. Mu, L. Fang, H. Yang, and X. Zhu, Europhys. Lett. **82**, 17009 (2008).
- [22] S. Liang, A. Moreo, and E. Dagotto, Phys. Rev. Lett. **111**, 047004 (2013); S. Liang, G. Alvarez, C. Sen, A. Moreo, and E. Dagotto, Phys. Rev. Lett. **109**, 047001 (2012).
- [23] C. Buhler, S. Yunoki, and A. Moreo, Phys. Rev. Lett. **84**, 2690 (2000).
- [24] M. Moraghebi, S. Yunoki, and A. Moreo, Phys. Rev. Lett. **88**, 187001 (2002).
- [25] D. Sénéchal, P.-L. Lavertu, M.-A. Marois, and A.-M. S. Tremblay, Phys. Rev. Lett. **94**, 156404 (2005).
- [26] A.M. Macridin, M. Jarrell, T. Maier, and G.A. Sawatzky, Phys. Rev. B **71**, 134527 (2005).
- [27] E. Dagotto, F. Ortolani, and D. Scalapino, Phys. Rev. B **46**, 3183 (1992).
- [28] Notice that $U_d \gg 16t$ is needed in order to destroy the $p-d$ hybridization.
- [29] In a future publication we will explore the case $\epsilon_p = 3.6$ eV with the p band above the d one, corresponding to a “negative charge-transfer gap” ($\Delta < 0$), following the choice in Ref. [4, 5] to emphasize the charge-transfer properties of the system ensuring that the doped holes go into almost pure p orbitals.
- [30] The magnitude of the localized spins is set to $S_i = 1$ since its actual value can be absorbed into the Hamiltonian parameters. This approximation prevents the consideration of the spin swap term studied in Ref. [17].
- [31] E. Dagotto, S. Yunoki, A. L. Malvezzi, A. Moreo, J. Hu, S. Capponi, D. Poilblanc, and N. Furukawa, Phys. Rev. B **58**, 6414 (1998).
- [32] S. Uchida, T. Ido, H. Takagi, T. Arima, Y. Tokura, and S. Tajima, Phys. Rev. B **43**, 7942 (1991).
- [33] G. Dopf, A. Muramatsu, and W. Hanke, Phys. Rev. B **41**, 9264 (1990).
- [34] Z.B. Huang, H.Q. Lin and J.E. Gubernatis, Phys. Rev. B **63**, 115112 (2001).
- [35] Y.F. Kung, C.-C. Chen, Yao Wang, E.W. Huang, E.A. Nowadnick, B. Moritz, R.T. Scalettar, S. Johnston, and T.P. Devereaux, Phys. Rev. B **93**, 155166 (2016).
- [36] S.R. White, Phys. Rev. Lett. **69**, 2863 (1992); Phys. Rev. B **48**, 10345 (1993).
- [37] The temperature T in Kelvin degrees is obtained using $T = 11, 605/\beta$.
- [38] A. Nazarenko, K.J.E. Vos, S. Haas, E. Dagotto, and R.J. Gooding, Phys. Rev. B **51**, 8676 (1995).
- [39] P. W. Leung, B. O. Wells, and R. J. Gooding, Phys. Rev. B **56**, 6320 (1997).
- [40] B.S. Shastry, Phys. Rev. Lett. **63**, 1288 (1989).
- [41] J.H. Jefferson, H. Eskes, and L.F. Feiner, Phys. Rev. B **45**, 7959 (1992).
- [42] C. Weber, K. Haule, and G. Kotliar, Phys. Rev. B **78**, 134519 (2008).
- [43] J. Graf, G.H. Gweon, and A. Lanzara, Physica C B **460**, 194 (2007).
- [44] D.S. Marshall, D. S. Dessau, A. G. Loeser, C-H. Park, A. Y. Matsuura, J. N. Eckstein, I. Bozovic, P. Fournier, A. Kapitulnik, W. E. Spicer, and Z.-X. Shen, Phys. Rev. Lett. **76**, 4841 (1996).
- [45] S.W. Cheong, G. Aeppli, T. E. Mason, H. Mook, S. M. Hayden, P. C. Canfield, Z. Fisk, K. N. Clausen, and J. L. Martinez, Phys. Rev. Lett. **67**, 1791 (1991).
- [46] P. Dai, H. A. Mook, and F. Dogan, Phys. Rev. Lett. **80**, 1738 (1998).
- [47] H.A. Mook, P. Dai, S. M. Hayden, G. Aeppli, T. G. Perring, and F. Dogan, Nature (London) **395**, 580 (1998).
- [48] J. M. Tranquada, J. D. Axe, N. Ichikawa, A. R. Moodenbaugh, Y. Nakamura, and S. Uchida, Phys. Rev. Lett. **78**, 338 (1997).
- [49] E. Berg, E. Fradkin, S.A. Kivelson, and J.M. Tranquada, New Journal of Physics **11** 115004 (2009).